XPS and Mössbauer Characterization of Au/TiO_2 Propene Epoxidation Catalysts

Aalbert Zwijnenburg,[†,‡] Anton Goossens,[§,||] Wim G. Sloof,[⊥] Menno W. J. Crajé,[§] Adri M. van der Kraan,[§] L. Jos de Jongh,[||] Michiel Makkee,*[,†] and Jacob A. Moulijn[†]

Industrial Catalysis, DelftChemTech, Faculty of Applied Sciences, Delft University of Technology, Julianalaan 136, 2628 BL Delft, The Netherlands, Interfacultair Reactor Instituut, Delft University of Technology, Mekelweg 15, 2629 JB Delft, The Netherlands, Kamerlingh Onnes Laboratorium, Universiteit Leiden, P.O. Box 9504, 2300 RA Leiden, The Netherlands, and Department of Materials Science and Technology, Faculty of Applied Sciences, Delft University of Technology, Rotterdamseweg 137, 2628 AL Delft, The Netherlands

Received: December 31, 2001; In Final Form: May 22, 2002

Gold catalysts supported on TiO_2 and TiO_2/SiO_2 were used in gas-phase propene epoxidation with a hydrogen−oxygen mixture. The catalysts were characterized by ^{197}Au Mössbauer absorption spectroscopy (MAS), X-ray photoelectron spectroscopy (XPS), and transmission electron microscopy (TEM). Gold particle sizes of 1 wt % Au catalysts calcined at 673 K ranged from 3 to 6 nm. Two Au contributions were found in Mössbauer spectra and assigned to bulk metallic Au atoms in the core of a gold particle and metallic gold on the outer surface of this particle. By MAS, no evidence for charge transfer from support to Au particle could be found. The Auger parameters confirmed that the surface layer of 3−5 nm gold particles is metallic. Deactivation is not due to a change in the active gold species but is related to the TiO_2 support. In the preparation via deposition-precipitation, $Au(OH)_3$ species are converted to metallic gold during calcination. Gold particles do not gradually grow during calcination, possibly due to the simultaneous conversion of $Au(OH)_3$ moieties with dehydroxylation of the TiO_2 support. Epoxidation activity increases with the amount of surface metallic gold. No evidence for oxidized gold under reaction conditions was found.

Introduction

Gold has traditionally been regarded as chemically too inert to be of any catalytic interest. However, it was found recently that, contrary to bulk gold, very small gold particles show exceptional catalytic activity.[1] The availability of new preparation routes and characterization techniques, like transmission electron microscopy (TEM), has led to new catalytic systems that show remarkable catalytic activity. For example, Haruta and co-workers showed that highly dispersed gold on a titania support is very active for CO oxidation at low temperature. They also reported that the same catalyst system can selectively produce propene oxide from propene, oxygen, and hydrogen.[2] These catalysts can be prepared by deposition−precipitation of $Au(OH)_3$ which typically yields 4−6 nm gold particles. Active Au/TiO_2-based propene epoxidation catalysts have typically a gold loading of up to a few wt % and give up to 2% propene oxide yield at >99% selectivity.[3] As the development of a direct gas-phase propene epoxidation process, comparable to that of ethene, is highly desired, a lot of effort is undertaken to understand this catalytic system and to come to new and/or improved catalysts.

The catalytic activity and selectivity of gold for epoxidation can be tuned by control of two major factors: selection of metal oxide supports and size of the gold particles.

Detailed studies highlighting the influence of the support on propene epoxidation with hydrogen and oxygen have been presented by Nijhuis et al.[3] and Mul et al.[4] They compared TiO_2, TiO_2/SiO_2, and titanium-silicalite-1 (TS-1). Nijhuis et al. propose a mechanism involving epoxidation of propene with a hydroperoxide-like species over a tetrahedral Ti site. Silica is not active in epoxidation, and as a consequence, Au/SiO_2 is not an active catalyst. Deactivation occurs over a TiO_2 support, whereas application of a dispersed titanium support (for example, TiO_2/SiO_2) prevents catalyst deactivation.[3]

It is claimed that in propene epoxidation gold is responsible for the formation of hydroperoxide-like species from H_2 and O_2.[3] In CO oxidation, the role of the gold is different: the (reducible) support supplies oxygen to the gold-support interface to react with CO that is adsorbed on gold.[5]

Haruta's work on propene epoxidation[2] indicates the existence of a critical size for gold in the reaction of propene with oxygen and hydrogen over Au/TiO_2 at a gold particle diameter around 2 nm. It is proposed that for gold particles larger than 2 nm propene oxide is selectively formed, whereas for particles smaller than 2 nm, only propane is formed.[2] A similar particle size effect was studied by Goodman and co-workers. From scanning tunneling spectroscopy (STS) experiments on Au/TiO_2 they found for decreasing particle size a metal to nonmetal transition at about 4 nm. Clusters of 3.2 nm were shown to exhibit the highest activity for CO oxidation.[6,7] Au/TiO_2-based catalysts consisting of gold in a (partially) oxidized state were

* To whom correspondence should be addressed. E-mail: m.makkee@tnw.tudelft.nl. Fax: +31-15-278-5006.
† Industrial Catalysis, DelftChemTech, Faculty of Applied Sciences, Delft University of Technology.
‡ Present address: Synetix, Steintor 9, D-46446 Emmerich, Germany.
§ Interfacultair Reactor Instituut, Delft University of Technology.
|| Universiteit Leiden.
⊥ Department of Materials Science and Technology, Faculty of Applied Sciences, Delft University of Technology.

10.1021/jp014723w CCC: $22.00
Published on Web 08/29/2002

recently claimed by Dow Chemical to be active in propene epoxidation.[8] The presence of oxidized gold was evidenced by XPS, TEM, and UV−vis studies.[8,9]

As stated above, an important aspect of the mechanism is the state of the gold atoms at the surface of the gold particle and at the gold−support interface. Several characterization techniques have been applied to elucidate the nature of the active site(s), like FTIR[10] and XPS,[11] but so far no conclusive answers have been found. The main challenge is the low concentration of gold in active catalysts. However, in general, an increase in gold loading will decrease the catalytic epoxidation activity, as higher gold loadings will usually result in larger gold particles.

In the present study, the nature of the active gold species in Au/TiO_2-based catalysts has been investigated by X-ray photoelectron spectroscopy (XPS) and ^{197}Au Mössbauer absorption spectroscopy (MAS). As it is element selective and sensitive to the local surroundings of the atoms, ^{197}Au MAS is an excellent probe, and successful studies have been carried out on Au/Fe-based systems[12,13] and, occasionally, on Au/TiO_2-based catalysts.[12−15] In addition, XPS has been used because of its surface sensitivity. Electron transmission spectroscopy (TEM) was used for determination of the particle size.

Experimental Section

Catalysts. Three 1 wt % gold catalysts have been prepared by static deposition−precipitation of $Au(OH)_3$ at a pH between 9.5 and 10.[3] $AuCl_3$ (Aldrich) dissolved in water was used as a gold source. As a support, TiO_2 (P25 Degussa), TiO_2/SiO_2 (prepared via reaction of titanium(IV)ethoxide (Fluka, 97%) in 2-propanol with surface hydroxyls of SiO_2 and calcination at 873 K[4]), and SiO_2 (Aldrich Davisil 646) were used.

Both a 1 and 10 wt % Au/TiO_2 have been prepared via a gold colloid route according to Grunwaldt et al.[16] using tetrakis-(hydroxymethyl)phosphonium chloride (THPC) as reductant and stabilizer. Furthermore, gold colloids were prepared based on a method by Porta et al.[17] using $LiBH_4$ as reductant and poly-(vinylpyrrolidone) (PVP) as stabilizer. For the colloid method, the required amount of TiO_2 was added to the colloid suspension, centrifuged, and washed at least three times with its own volume with distilled water to yield a Au/TiO_2 catalyst. Again, both 1 and 10 wt % Au catalysts were prepared. The samples were dried at 368 K for 8 h prior to calcination.

All catalysts have been calcined under static conditions at 673 K unless stated otherwise.

Characterization. Transmission electron microscopy (TEM) was employed to determine the gold particle size. A Philips CM30T electron microscope with a LaB_6 filament as the source of electrons was operated at 300 kV. Samples were mounted on a microgrid carbon polymer supported on a copper grid by placing a few droplets of a suspension of ground sample in ethanol on the grid, followed by drying at ambient conditions.

For the ^{197}Au MAS measurements, the applied ^{197}Au γ-ray sources were obtained by irradiating enriched platinum powder (97.4% ^{196}Pt) with thermal neutrons for 24 h in the nuclear reactor of the Interfacultair Reactor Instituut, Delft, The Netherlands. This resulted in a 200 MBq Mössbauer source due to the $^{196}Pt(n, \gamma)^{197}Pt$ reaction. The subsequent beta-decay process to the Mössbauer isotope ^{197}Au has a half-life of 18.3 h, which determines the half-life of the ^{197}Au Mössbauer source. Mössbauer spectra have been recorded in transmission geometry. Both source and absorber were cooled to a temperature of 4.2 K unless stated otherwise. For detection of the transmitted photons, a high purity Ge detector has been used. The source velocity has been calibrated by a Michelson interferometer. All IS values are given according to this (absolute) scale. For the data analysis, the peak position of the bulk gold contribution was fixed at −1.22 mm/s (the reference value obtained for metallic bulk gold), unless stated otherwise. Further details on the analysis procedures are given in the corresponding table captions.

X-ray photoelectron spectroscopy (XPS) was employed to determine the chemical state of the surface gold atoms of the catalysts. To this end, not only the value of the binding energy of the Au $4f_{7/2}$ electrons was considered but also the so-called Auger parameter[18] by analyzing the Au $M_5N_{67}N_{67}$ electrons. In particular, the value of the Auger parameter reflects the chemical environment of the Au atom without being effected by sample charging or Fermi-level shifts. For the XPS analysis, samples were prepared from the Au/TiO_2 catalysts by pressing the material into a soft indium foil (Alfa Products UK, 99.9975% In) on a flat specimen holder. XPS spectra of Au 4f, O 1s, C 1s, and Ti 2p photoelectron lines and the Au $M_5N_{67}N_{67}$ Auger line were recorded with a PHI 5400 ESCA instrument with a step size of 0.1 eV. The instrument was set at a constant analyzer pass energy of 35.75 eV and unmonochromatized incident Mg X-ray radiation (Mg $K\alpha_{1,2}$ = 1253.6 eV) was used. The Au $M_5N_{67}N_{67}$ Auger electrons with a kinetic energy of about 2015 eV can only be generated with the "Bremsstrahlung" produced by the X-ray source operating at 15 kV and 400 W using the Mg anode. Therefore, the Auger line is recorded at an apparent negative binding energy.[19] The energy scale of the spherical capacitor analyzer (SCA) spectrometer was calibrated according to a procedure described in the literature.[20] The electrons emitted from the sample were detected at an angle of 45° with respect to the sample surface. An elliptic area of 1.1 × 1.6 mm was analyzed. As a reference for metalic Au, spectra were recorded from a film of pure Au, obtained after sputter cleaning with 4 keV Ar^+ ion beam rastering an area of 5 × 5 mm for 10 min.

To exclude any effects on the values of binding energies due to charging of the sample during the XPS analysis, all data are corrected by a linear shift such that the peak maximum of the main line in the C 1s spectra corresponds with 284.8 eV. The photoelectron binding energies (BE) and the Auger electron kinetic energies were determined from the spectra by taking the value corresponding with the peak maximum after a 7-points Savitzky−Golay smoothing of the signal.

The Auger parameter α of Au in the 10 wt % Au on TiO_2 samples has been determined by using the formula:[18,21]

$$\alpha = \mathrm{BE}(\mathrm{Au}\ 4f_{7/2}) + \mathrm{KE}(\mathrm{Au}\ M_5N_{67}N_{67}) \qquad (1)$$

In this equation, BE(Au $4f_{7/2}$) is the binding energy of the Au $4f_{7/2}$ electrons, and KE(Au $M_5N_{67}N_{67}$) the kinetic energy of the Au $M_5N_{67}N_{67}$ Auger electrons.

For determination of the epoxidation activity, steady-state experiments were performed in a microflow setup. In this setup nitrogen (70 vol %), oxygen (10 vol %), hydrogen (10 vol %), and propene (10 vol %) were continuously fed over a 10 mL fixed-bed reactor placed in a fluidized-bed oven. The weight hourly space velocity (WHSV) was 0.71 $g_{propene}/g_{cat}$ h. The analysis of the reaction products was performed using an automated sampling gas chromatograph, analyzing a gas sample every 12 min. A Poraplot Q 0.53 mm diameter, 25 m length capillary column was used with He as carrier gas. A flame ionization detector (FID) was used for the analysis. The hydrogen and oxygen consumption could be measured on the same gas chromatograph using a Molsieve 5 Å, 2 mm diameter, 3 m length column, and a TCD detector.

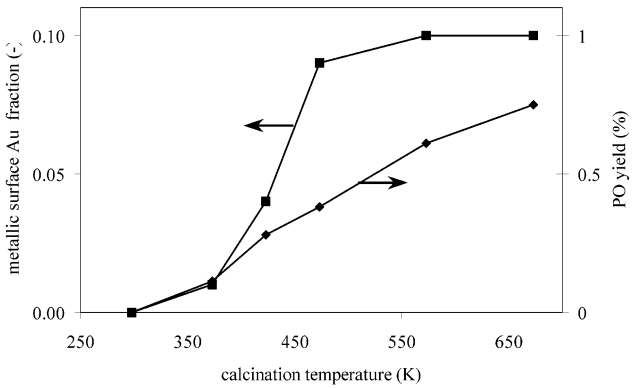

Figure 1. PO yield (% of propene feed) and fraction of metallic surface gold species in the Mössbauer spectrum as a function of calcination temperature of Au/TiO_2 catalyst. Reaction data were taken after 2 h on stream at 323 K. Under these conditions, less than 5% of the initial activity of the Au/TiO_2 is lost due to deactivation.

Results

In previous work, propene epoxidation catalysts have been prepared by deposition−precipitation of $Au(OH)_3$ at a pH between 9.5 and 10 on TiO_2-based supports.[3] In a standard preparation procedure, these samples are washed to remove Cl^- ions and subsequently subjected to calcination at 673 K. To investigate the influence of Cl^- on the gold, both washed and unwashed samples are tested in the gas-phase epoxidation reaction. Furthermore, a stepwise calcination of the washed samples is performed, whereby after each calcination step the epoxidation activity has been determined. Propene oxide (PO) yields over these stepwise calcined Au/TiO_2 samples are recorded after 2 h reaction time at 323 K. PO is the only product observed, and in Figure 1, the PO yield is given as a function of the calcination temperature. The noncalcined samples (both washed and unwashed) are not active in the epoxidation reaction, but the activity of the washed samples increases with calcination temperature. During calcination, the white samples turn into their characteristic purple color, which is indicative of the presence of small particles of metallic gold.[24]

After each calcination step, a Mössbauer spectrum of these 1 wt % Au/TiO_2 samples is recorded. The spectra as given in Figure 2a are fitted with in total four gold species with fixed IS (isomer shift) and QS (quadrupole splitting). The analysis results are given in Table 1. The spectra of the noncalcined samples can be described with two contributions with large IS and QS values. For both spectra after calcination of 373 and 423 K, a misfit can be observed in Figure 2 (in the 3−6 mm/s range on the velocity axis), which indicates that the IS-QS parameters of the two contributions slightly change during calcination. In fact, doublets with slightly different (IS,QS) would give better analyses. If the IS and QS positions are not fixed, the IS of the third contribution (Table 1) is decreased from 2.4 mm/s without calcination to 2.2 mm/s after calcination at 373 and 423 K, respectively. These two contributions decrease in intensity during calcination, and at 573 K and higher calcination temperature, the spectrum consists of two other contributions with lower IS. The peak at IS and QS of −1.22 and 0 mm/s, respectively, is fixed at the position of the Au foil reference. At calcination temperatures above 473 K the spectrum is largely determined by this so-called bulk gold contribution. The increase in relative intensity of this bulk gold contribution with increasing calcination temperature is accompanied by an increase in intensity of the contribution at IS and QS of −1.26 and 2.69 mm/s, respectively. This latter contribution is also given in Figure 1 as a function of calcination temperature.

In Figure 2b the corresponding TEM micrographs are given. No gold particles are observed on the noncalcined washed sample, also not under prolonged exposure to the electron beam (not shown), although the TiO_2 crystals become more amorphous. Metallic gold particles (dark spots in the micrographs) appear after calcination at 373 K. Surprisingly, the particles do not increase in size but only in number during the calcination procedure. The formation of metallic gold particles seems to proceed inhomogeneously throughout the TiO_2 sample, which is confirmed by visual inspection of the sample calcined at 373 K. Both white and light purple support particles can be observed separately. During calcination at 423 K and higher temperatures, the sample becomes more purple and at the same time homogeneous by color (all particles have the same color). Several parts of the samples were inspected, and it appeared that the individual samples were rather homogeneous. Therefore, no statistical analysis was required.

The Mössbauer spectrum of the 1 wt % Au/TiO_2 catalyst (calcined at 673 K) is given in Figure 2 (bottom spectrum). In Figure 3 and Table 2, MAS data of this fully calcined catalyst are compared with MAS data of 1 wt % Au on a TiO_2/SiO_2 and on a SiO_2 support. A preliminary report on these three spectra has been published previously.[22] The spectra typically consist of a predominant bulk gold contribution (IS = −1.22 mm/s, QS = 0 mm/s). Besides the bulk gold contribution, one other Au species is found with varying IS and QS. The spectral contribution of this second Au species is depending on the support. TEM analysis of these catalysts (not shown) was carried out to determine the average gold particle sizes. Gold particle sizes stated in Table 2 are depending on the support and the observed sizes in good agreement with previously reported results.[3] The TiO_2 and TiO_2/SiO_2-based catalysts show a small particle size distribution ($2\sigma \approx 2$ nm), but for the Au/SiO_2, a broad particle size distribution is found in the form of large agglomerates (up to 30 nm in size), consisting of primary Au particles about 6 nm in diameter. For the Au/SiO_2, no statistical analysis was performed due to the limited number of gold particles observed and the number of micrographs taken. As already pointed out by Nijhuis and co-workers,[3] the 1 wt % Au on TiO_2/SiO_2 catalyst shows 1.0% propene oxide (PO) yield with >99% selectivity at 373 K. The TiO_2 based catalyst is already active at 323 K, where propene conversion to PO is 0.8% at >99% selectivity (Figure 1). The Au/SiO_2 catalyst is not active in epoxidation. [3]

As reported in the literature,[3,4] the Au/TiO_2 catalyst shows deactivation after several hours on stream above 348 K. The Au/TiO_2 catalyst was subjected to the epoxidation reaction at 348 K and showed only 25% of its initial PO yield after 10 h on stream, maintaining >99% selectivity and a constant water production over the investigated time interval. Subsequently, its Mössbauer spectrum was recorded and it is given in Figure 3. TEM analysis (not shown) did not indicate sintering of the gold particles, and the spectral contributions (Table 2) are in good agreement with the fresh Au/TiO_2 sample.

XPS measurements have been carried out on some of the Au/TiO_2 samples. The two Au/TiO_2 samples calcined at 673 and 423 K and the spent Au/TiO_2 have been analyzed and the Au 4f lines are given in Figure 4. The Au $4f_{7/2}$ BE (binding energy) is given in Table 3. The C 1s line position is used as a reference, which results in negative Au $4f_{7/2}$ BE shifts of up to 0.7 eV relative to the 84.00 eV value for metallic gold.[23] Clearly, it can be seen that the Au 4f BE of Au/TiO_2 calcined at 673 K does not change much after propene epoxidation reaction. For the spent Au/TiO_2 catalyst, two C 1s peaks (not shown) are

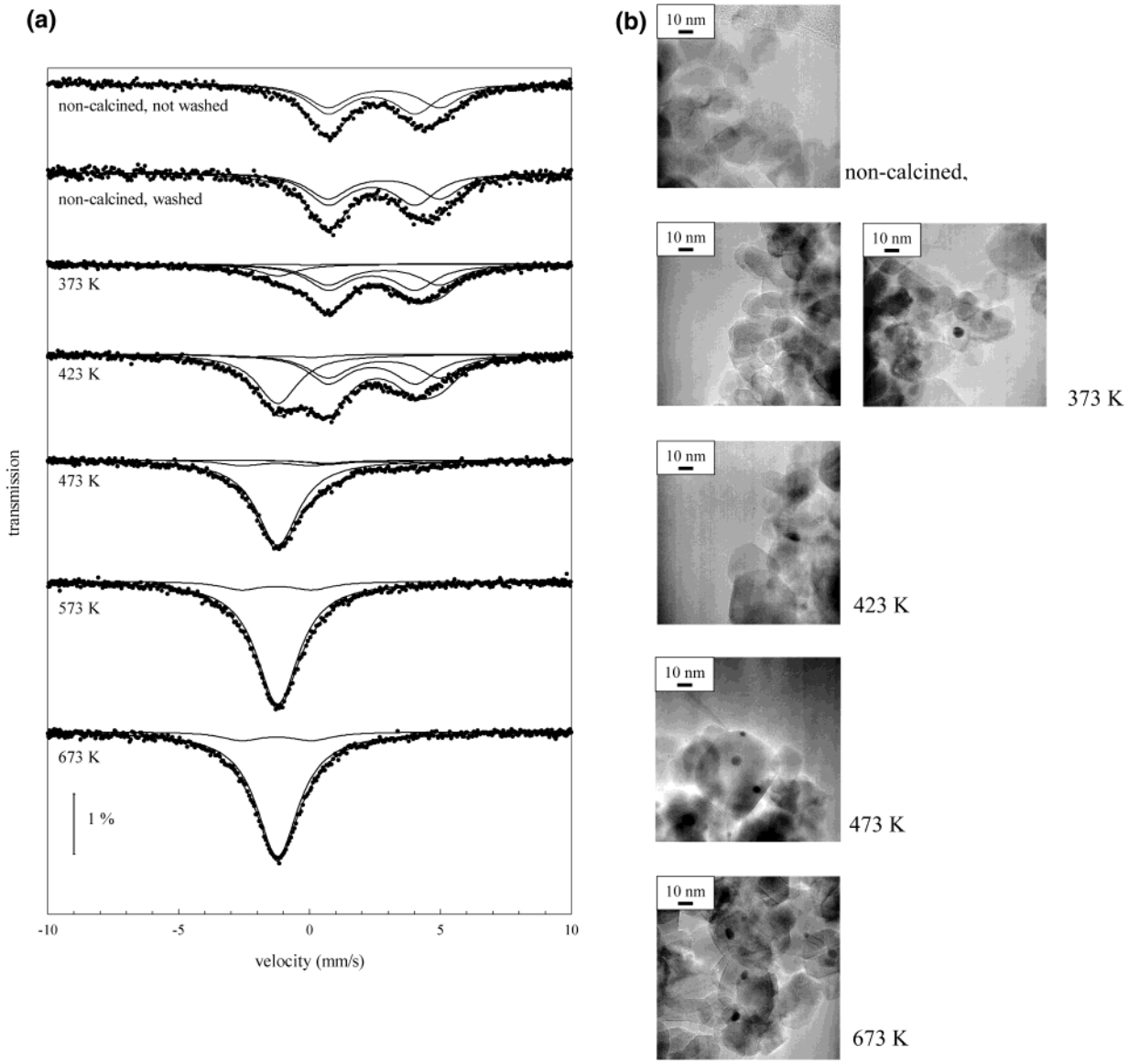

Figure 2. (a) MAS spectra of Au/TiO_2 catalyst a function of calcination temperature. Spectra were recorded at 4.2 K and have been fitted with four sets of (IS,QS) values. The spectra are given in the same intensity scale but vertically shifted. (b) TEM micrographs of the Au/TiO_2 samples calcined at the temperatures as given in the insert.

TABLE 1: Relative Intensity (%) of the Four (IS,QS) Contributions in the Mössbauer Spectra of 1 wt % Au/TiO_2 at Different Calcination Temperatures

Au/TiO_2 calcination temperature (K)	intensity of (IS,QS) contribution (%)			
	(−1.22, 0)	(−1.26, 2.69)	(2.38, 3.32)	(2.84, 4.27)
noncalcined, not washed			55	45
noncalcined, washed			55	45
373	12	1.0	48	39
423	32	4.0	35	29
473	79	9.0	7.0	5.0
573	89	10	0.55	0.45
673	90	10		

observed, the second peak has 1.45 eV higher BE than the first peak of the usual hydrocarbon impurity. In Figure 4 and Table 3, it can be seen that the Au/TiO_2 sample calcined at 423 K has a higher BE of about 0.9 eV compared to the sample calcined at 673 K. The Auger signals for 1 wt % Au samples are too weak to be observed. Therefore, higher gold loaded samples were additionally prepared using a different preparation method.

In Figure 5, TEM micrographs of the four catalysts prepared via the colloid routes are given. Both the 1 and 10 wt % Au/TiO_2 catalysts prepared using tetrakis(hydroxymethyl)phosphonium chloride (THPC) as stabilizer and reductant yield gold particles in a narrow size range around 5 nm (4−6 nm), independent of gold loading. However, these samples are not active in the epoxidation reaction, as shown in Figure 6. Using poly(vinylpyrrolidone) (PVP) as stabilizer and $LiBH_4$ as reductant, Au particles with a similar mean particle size appear on the support of both 1 and 10 wt % samples. The distribution of particle sizes (3−10 nm) turned out to be somewhat larger than that observed for the THPC sample. For the 10 wt % PVP sample also, a few 15 nm agglomerates consisting of 5 nm primary particles were observed. However, the overall particle size is reasonably uniform, and the mean particle size is comparable to the THPC-based catalysts. The resulting PVP catalysts are both active and selective in propene epoxidation.

Using XPS, no profound differences in C 1s intensities of these 10 wt % Au samples (not shown) were observed,

TABLE 2: Mean Gold Particle Sizes (Including Standard Deviation) as Determined by TEM and (IS, QS) of the Two Contributions in the Mössbauer Spectra of 1 wt % Au Catalysts on Different Supports[a]

sample	size (nm)	IS (mm/s)	QS (mm/s)	intensity (%)	IS (mm/s)	QS (mm/s)	intensity (%)
Au/TiO_2 673 K	5.2 ± 1.1	−1.22	0	90	−1.26	2.69	10
Au/TiO_2 673 K spent	5.2 ± 1.1	−1.22	0	90	−0.64	1.77	10
Au/TiO_2/SiO_2 673 K	3.2 ± 0.98	−1.22	0	78	−1.09	2.52	22
Au/SiO_2 673 K	6	−1.22	0	66	−0.98	2.58	34

[a] One contribution was fixed at (−1.22, 0) mm/s. The relative intensity of the contributions is also given. All samples were calcined at 673 K. The Au/TiO_2 catalyst was both tested before and after epoxidation reaction (spent).

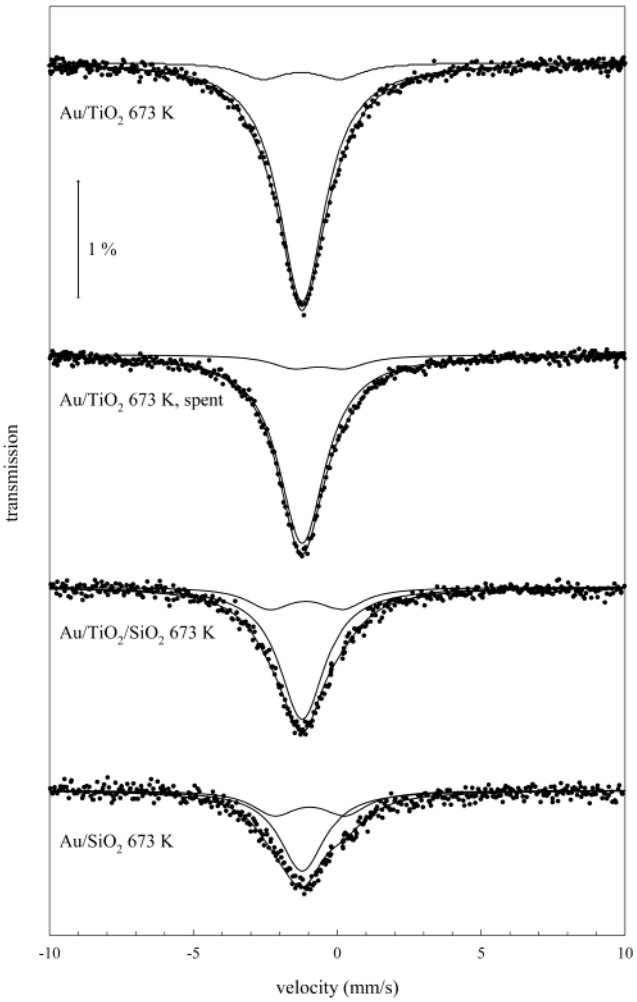

Figure 3. MAS spectra of fresh Au/TiO_2 catalyst compared to Au/TiO_2 after reaction spent, Au/TiO_2/SiO_2, and Au/SiO_2. All catalysts had a 1 wt % Au loading and were calcined at 673 K. The spectra were recorded at 4.2 K and have been fitted with two gold contributions, one with IS being fixed at −1.22 mm/s and one with varying (IS,QS). The spectra are given in the same intensity scale but vertically shifted.

indicating that calcination at 673 K removes all hydrocarbon impurities remaining from the stabilizers used in the colloid synthesis. A P $2p_{3/2}$ peak in the XPS spectrum has been observed at BE 133.8 eV for the 10 wt % Au/TiO_2 (THPC) sample, which corresponds to either phosphate or Au−P complexes.[23]

For the 10 wt % Au/TiO_2 catalysts, the Auger parameters were determined from the Au 4f XPS and the Au $M_5N_{67}N_{67}$ Auger peaks as given in Figure 7. The relevant parameters are given in Table 3. For comparison, also the spectra of the gold film reference are reported. All signals were smoothed before the peak maximum was determined. This gave less than 0.05 eV change in BE for the Au reference peak as determined with and without smoothing. The Au 4f spectra of the two 10 wt %

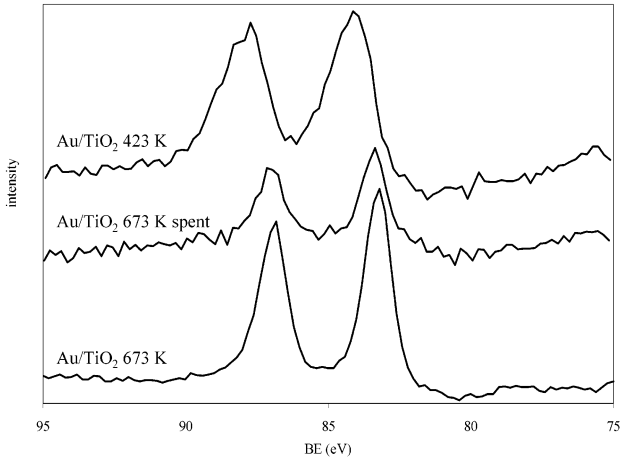

Figure 4. XPS spectra of 1 wt % Au/TiO_2 samples, from bottom to top: Au/TiO_2 calcined at 673 K, same catalyst after propene epoxidation reaction, and Au/TiO_2 calcined at 423 K.

TABLE 3: Au $4f_{7/2}$ Binding Energy and Au $M_5N_{67}N_{67}$ Kinetic Energy with Reference to C 1s at 284.8 eV for Different Au Catalysts and the Au Reference Material[a]

sample	BE (Au $4f_{7/2}$) (eV)	KE (Au $M_5N_{67}N_{67}$) (eV)	α (eV)
1 wt % Au/TiO_2 673 K	83.29		
1 wt % Au/TiO_2 673 K spent	83.30		
1 wt % Au/TiO_2 423 K	84.21		
10 wt % Au/TiO_2 (THPC)	83.47	2015.61	2099.08
10 wt % Au/TiO_2 (PVP)	83.49	2015.39	2098.88
Au reference	84.05	2015.10	2099.15

[a] The Auger parameter α has been determined from the Au $4f_{7/2}$ binding energy and Au $M_5N_{67}N_{67}$ line positions (see text for details).

catalysts clearly show a shift to lower BE compared to the Au reference. The Auger parameter α of Au in the 10 wt % Au on TiO_2 samples has been determined by use of eq 1. These α values are given in Table 3 relative to the value determined for the Au reference. The table shows for both samples a small negative shift in Auger parameter compared to the Au film reference.

Discussion

Bulk and Surface Gold Species Observed by MAS. Combinations of IS (isomer shift) and QS (quadrupole splitting) are indicative of the oxidation state of gold. In Figure 8, the obtained (IS,QS) combinations are summarized. Literature values of several gold compounds containing Cl, O, and gold colloids are also shown for comparison. To illustrate the reliability of the MAS method, IS and QS values of $HAuCl_4$ were taken from the literature[13] as well as experimentally determined. The maximum difference in IS and QS was only 0.2 mm/s. The lines in Figure 8 correspond to the region in which usually Au compounds with two-coordinated planar (Au^{I}) or four-coordinated square-planar (Au^{III}) appear.[25]

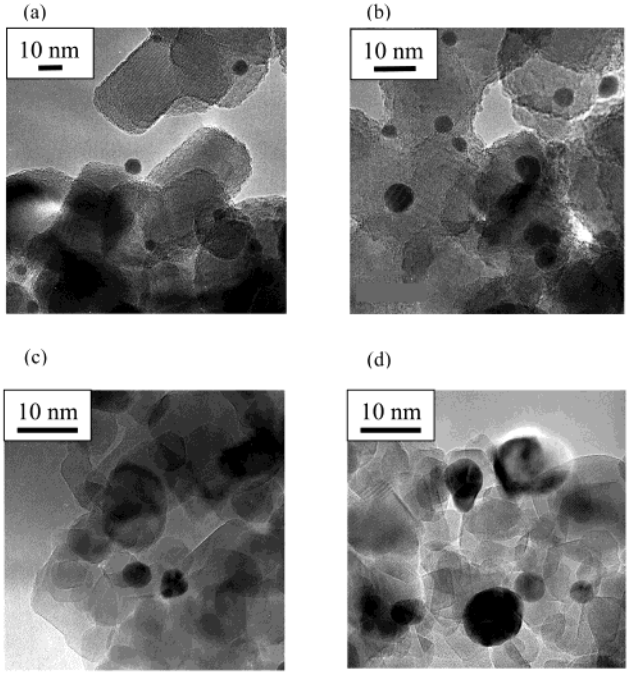

Figure 5. TEM micrographs of 1 (a and c) and 10 (b and d) wt % Au/TiO_2 catalysts prepared via a colloid synthesis route: a and b using colloid route via tetrakis(hydroxymethyl)phosphonium chloride (THPC) and c and d using colloid route via poly(vinylpyrrolidone) (PVP).

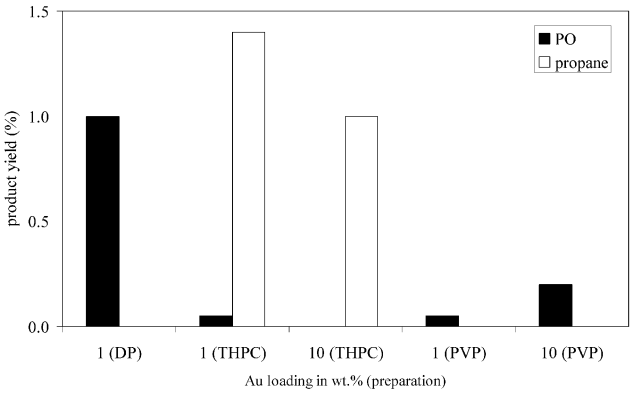

Figure 6. PO and propane yield (% of propene feed) as a function of gold loading and preparation route. DP = deposition-precipitation, THPC = colloid route via tetrakis(hydroxymethyl)phosphonium chloride, and PVP = colloid route via poly(vinylpyrrolidone). Reaction data were taken after 30 min on stream at 348 K. Under these conditions less, than 5% of the initial activity of the Au/TiO_2 is lost due to deactivation.

The spectra of both the washed and unwashed $Au(OH)_3/TiO_2$ samples consist of two contributions, viz., at (IS,QS) of (2.38,3.32) and (2.84,4.27). The IS−QS parameters for the two species are well in the range of what is usually measured for Au^{III} compounds, but both IS and QS are higher than reported in the literature for Au^{III}−oxyhydroxide[13] and Au_2O_3.[26] These literature values show that both IS and QS increase going from Au_2O_3 to AuO(OH). Therefore, probably, the two species observed for noncalcined wet samples are both due to $Au(OH)_3$ supported on TiO_2. The (IS,QS) sets of the two species are in good agreement with the two species found for $Au(OH)_3$ on $Mg(OH)_2$ as reported by Kobayashi et al.[14] Furthermore, based on the comparison of both washed and unwashed noncalcined samples, it can be concluded that the presence of Cl^- has no detectable influence on the gold atoms. In other words, it is likely that only $Au(OH)_3$ and not a gold chlorohydroxy species is deposited on the TiO_2 support at room temperature and pH 9.5−10. At this high pH, the existence of chlorohydroxy species is unlikely, which is also supported by the literature.[2,27]

When calcined up to a calcination temperature of 423 K, the two just-mentioned Au^{III} species gradually decrease in intensity. From 373 K onward, two other contributions appear in the spectra. One contribution is predominant and has IS = −1.22 mm/s and no quadrupole splitting. This peak is fixed at the values obtained for the gold foil reference and is assigned to metallic (bulk) gold. The presence of metallic gold particles is also supported by the observation that this sample is light purple after calcination at 373 K. In agreement with MAS studies on Au clusters of similar size available in the literature,[28−31] this contribution is assigned to gold in the core of a metal particle and further denoted as bulk gold.

Comparison of the data with different supports as given in Figure 3 shows that the spectra in all cases exhibit a predominant bulk gold contribution at (IS,QS) = (−1.22,0). Apparently, the gold in the core of the particle is not influenced by the support. In principle, the IS value of the gold atoms in the cores of the particles are dependent on the chemical nature of the gold atoms on the surface of the particle. However, if there are delocalized electrons present in the metal core, the influence of the surface gold atoms on the core atoms will be greatly reduced. This electronic screening effect is very effective over short distances.[29] As expected, because the Au/TiO_2-based samples used in this study have a mean gold particle size of more than 3 nm (about 10^3 atoms), the electronic screening of core atoms is perfect, and an IS value for core atoms indistinguishable from bulk gold is observed.

The other contribution at (IS,QS) of (−1.26,2.69) observed at higher calcination temperatures appears to be also present for gold supported on TiO_2/SiO_2 and SiO_2, with an IS and QS of -1.1 ± 0.1 and 2.6 ± 0.1 mm/s, respectively. As can be seen in Figure 8, the observed IS-QS combinations close to values obtained from spectra of 1.5−6 nm Au metal particles in a Mylar matrix as reported by Stievano and co-workers.[31] These researchers assign these contributions to surface atoms of gold particles. Furthermore, other reports in the literature[29,30] indicate that spectra of gold particles can usually be described by a metallic core of identically coordinated atoms and a contribution from the surface shell of one atom layer thick. In line with these interpretations, the second contribution found in this study at (IS,QS) = (-1.1 ± 0.1, 2.6 ± 0.1) is assigned to the surface atoms. In Figure 1, it is shown that the increase in PO yield nicely correlates with the increase of the fraction of these surface atoms.

The relative intensity of this surface species is given as a function of the particle size in Figure 9. In this figure also, the fraction of surface Au atoms is calculated assuming hemispherical gold particles[1] and a recoil-free fraction (f-factor) of 0.04 compared to the bulk gold value of 0.189. In the study by Paulus et al.,[30] a ratio of 1.35 between f factor for bulk and surface gold species (0.189/0.14) for 6−17 nm gold colloids was reported. The lower f factor of Au atoms on the surface of the particle (0.04 vs 0.14 as observed by Paulus et al.[30]) can be attributed to their lower coordination and the absence of ligands. The f factor of the surface atoms would be higher if the Au atoms that form the contact between gold and support would also be treated as "surface" atoms. However, these atoms on the boundary of gold particle and support are expected to exhibit (slightly) different MAS parameters (IS around −1.22, QS in the 1−3 mm/s range for metallic species), and this is not observed experimentally. These atoms either are present in low

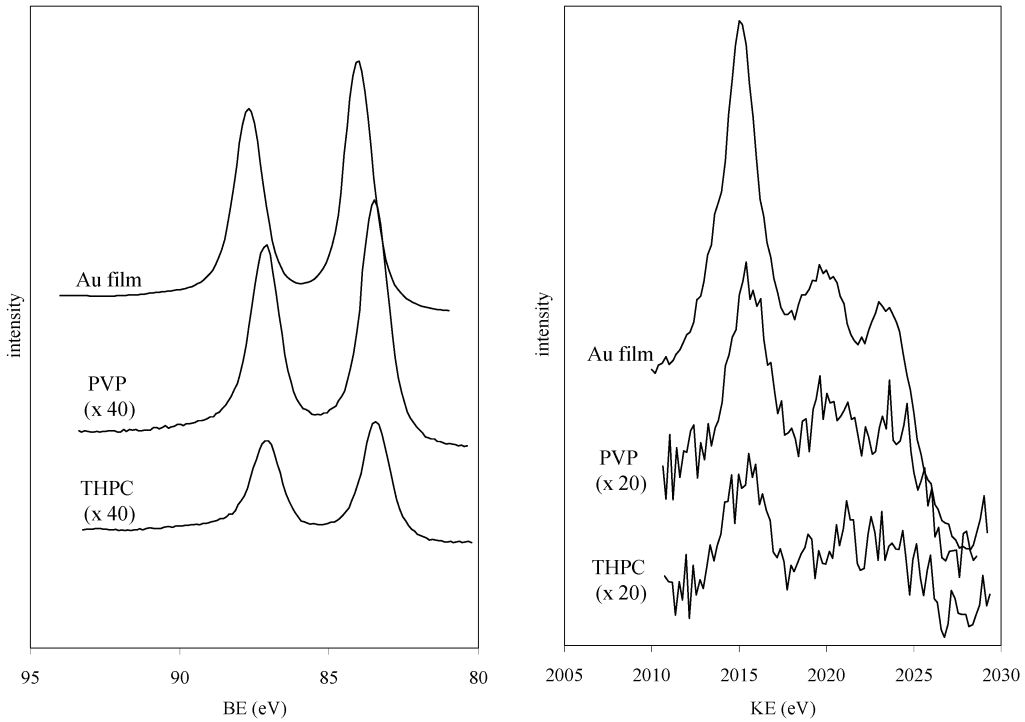

Figure 7. XPS spectra of Au 4f (left) and Auger $M_5N_{67}N_{67}$ (right) for 10 wt % Au on TiO_2 catalysts prepared via THPC or PVP route compared to Au reference (Au film). BE = binding energy, KE = kinetic energy

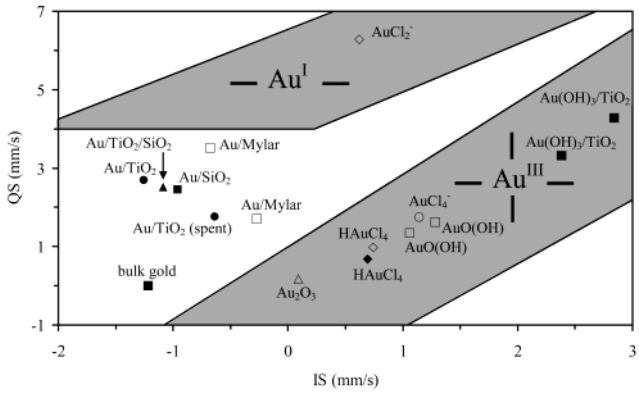

Figure 8. IS and QS plot of propene epoxidation catalyst data (closed symbols) compared to literature values (open symbols, Au/Mylar,[31] Au_2O_3,[26] and other Au compounds[13]). Lines indicate the regions in which Au^I/Au^{III} compounds are usually reported.[25] IS and QS combinations denoted as $Au(OH)_3/TiO_2$ are the two contributions found for the noncalcined TiO_2 samples of Figure 2. Catalysts calcined at 373 K and higher consist of two contributions: bulk gold and a contribution depending on support (TiO_2, TiO_2/SiO_2, and SiO_2 as given in Figures 2 and 3). Furthermore, the (IS,QS) of a spent Au/TiO_2 (taken from Figure 3) catalyst is given.

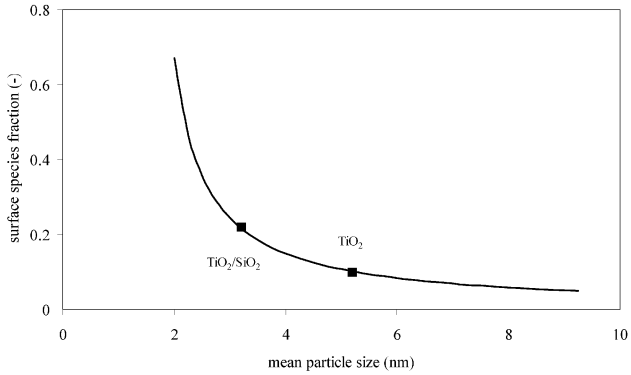

Figure 9. Fraction of Au surface species on different supports plotted versus mean particle size determined by TEM. The line represents the fraction of surface atoms calculated by assuming hemispherical gold particles and an surface atoms f factor of 0.04 compared to the bulk value of 0.189.

concentration (leading to low spectral intensity) or not much different from the bulk gold species in the core of the metal particles.

The data for the Au/SiO_2 sample are not shown in Figure 9, as for this sample a broad particle size distribution is observed by TEM. Large agglomerates up to 30 nm in size consisting of about 6 nm primary Au particles are found. The definition of a mean particle size is, therefore, not possible.

The main question regarding the surface species is whether they can be attributed to oxidized gold species or not. As described in the Experimental Section, the IS yields information on the valence state of the gold, whereas the QS gives information on the coordination of the neighboring atoms. In Figure 8, it can be seen that IS values for the surface contributions (-1.1 ± 0.1 mm/s) are concentrated around the value of bulk Au (-1.22 mm/s). Furthermore, Figure 8 shows that the IS-QS combinations of the surface species do not fit within the regions that are known for the ionic Au^I or Au^{III} species. The observed behavior of the surface sites can thus be explained in terms of a metallic surface layer with an IS value close to bulk gold and QS values depending on the symmetry of the local coordination of the surface atoms. This interpretation of the spectra agrees with the investigations on Au and Pt clusters and colloids that showed that surface sites can best be described as disturbed but metallic atom shells.[29,30]

In conclusion, MAS spectra of 1 wt % Au on different supports indicate that Au particles of about 5 nm in size can be described by a bulk gold and a surface species contribution. No separate contribution of the atoms on the boundary between Au particle and support is observed. Either, these boundary atoms are present in a too small amount to be detected or their MAS parameters are not much different from those of the bulk gold or the surface species. The last option would rule out the

presence of Au^{III} atoms as "chemical glue" between the Au metal particle and the support, as proposed by Bond and Thompson[32] for CO oxidation catalysts.

Deactivation of Au/TiO_2. TEM indicates that the deactivation observed for $Au/TiO_2$3 is not due to sintering of gold particles. Furthermore, the intensity ratio of bulk versus surface species (90:10) as found by MAS (Table 2) for the spent catalyst is identical to that observed for the fresh sample. Sintering is also not to be expected at the reaction temperature of 348 K, as the catalyst was already calcined at 673 K. The small deviations in IS and QS of fresh and spent Au/TiO_2 samples might be attributed to small changes in valence state/coordination of surface atoms. Further information on the source of the deactivation comes from in-situ-IR spectroscopy,[4] which showed that deactivation takes place at Ti−oxide sites rather than on Au sites, and the observation that the rate of water production of a deactivated Au/TiO_2 remains constant. The latter is in good harmony with the previously proposed mechanism based on an OOH-like species over gold, which may be the intermediate in water formation.[3]

Gold Phases Observed during Preparation of Active Epoxidation Catalysts. Both MAS and TEM indicate that reduction of $Au(OH)_3$ to metallic gold, bulk, and surface Au takes place and that the particles do not grow gradually in size, during calcination. Furthermore, TEM analysis indicates that $Au(OH)_3$ is highly dispersed. As a uniform gold particle size distribution is obtained during calcination, a homogeneous deposition of $Au(OH)_3$ species is not to be expected, as this would lead to a broad particle size distribution. Also based on the deposition−precipitation chemistry,[33] the presence of discrete islands of $Au(OH)_3$ (of typically less than 1 nm thickness) is more likely. Blick and co-workers observed moiré fringes of up to 20 nm for 0.04 wt % Au/MgO catalysts that were assigned to two-dimensional surface patches of oxidized gold. They observed (IS,QS) of (1.38,0) mm/s of these species that confirmed their assumption. These patches were mobile under the influence of the electron beam and tended to disappear within a few seconds.[34] This may explain the difficulty of observing the $Au(OH)_3$ species of this study in TEM.

These thin $Au(OH)_3$ islands are not active in propene epoxidation, and Figure 1 clearly shows that the PO yield is correlated with the presence of metallic gold. The observation that, although above 573 K the amount of surface Au is constant, the activity still slightly increases with calcination temperature might be related to the degree of hydroxylation of the Ti−oxide surface. The importance of hydroxylation has been mentioned in the literature.

Haruta and co-workers[35] found for Au/Fe_2O_3 catalysts that the formation of metallic gold was accompanied by the conversion of ferric hydroxide to crystalline Fe_2O_3. Furthermore, Park and Lee[36] observed that oxidized gold of a catalyst calcined at 373 K could be stabilized during CO oxidation at 310−330 K for both Au/Fe_2O_3 and Au/Al_2O_3 catalysts operating under wet conditions. As MAS is element-selective, it is an excellent probe to study the coordination and oxidation states of gold species. However, the active epoxidation catalysts studied here have particles larger than 3 nm, and the gold surface atoms contribute typically 10% to the spectrum. The active gold site, which can be located at or near the Au−support interface might, therefore, not be visible in the Mössbauer spectrum. Furthermore, charging of the Au particle due to interaction with the support will not have a large influence in the Mössbauer spectrum. For gold particles larger than 55 atoms, a shift in IS of less than 0.1 mm/s has been calculated upon charging by the addition of one electron.[37] Therefore, XPS analysis was carried out, as it is more surface sensitive.

Oxidized or Metallic Gold Surface Layer Responsible for Propene Epoxidation? The interpretation of Au 4f binding energies (BE) as determined by XPS is still subject of debate with respect to metal−support interaction (charging of the metal particle) and particle size effects.[7] As metallic gold has a BE of 84.00 eV,[23] higher BEs (positive shifts) are usually assigned to (partially) oxidized gold. However, Table 3 clearly shows *lower* BE values for different 1 wt % Au/TiO_2 samples.

In the literature, negative shifts in Au 4f BE have been observed before and explained by electron transfer to the gold. For 7.5−12.5 nm Au particles supported on Fe_2O_3, Guczi et al.[38] found a decrease in BE from 84.3 to 83.9 eV upon oxidation of the catalyst. These researchers concluded that $Au^{\delta+}$ was converted to $Au^{\delta-}$ by charge-transfer involving O_2 species.[38] Electron-rich gold species were proposed by Claus et al. to play a role in the hydrogenation of acrolein over 1 nm gold particles on TiO_2, based on electron spin resonance (EPR) studies.[39]

Besides the oxidation state, for nanosized particles, both initial and final state effects can cause shifts in BE. The initial state effect involves a decrease in BE with a decrease in gold particle size, because of the increased number of surface atoms. Surface atoms have less neighbors than bulk atoms, which decreases the surface valence-band width. Therefore, the Au 5d electrons are more localized, and this decreases the Au 4f BE.[40,41] Final state effects involve an increase in BE with a decrease in gold particle size. Smaller particles have more discrete conduction bands and more surface atoms with reduced coordination. Upon creation of a core hole by the incoming X-ray, the screening of this hole will be less for smaller particles. Therefore, the photoelectron will experience a higher BE. Both initial and final state effects are influenced by charging. Charging is dependent on the ability of the support to neutralize the particle within the lifetime of the core hole.[40]

First, the validity of the C 1s reference was checked. Using C 1s as reference may lead to small shifts in Au $4f_{7/2}$ BE because of the presence of C−O as well as C−C bonds on TiO_2 supported catalysts.[4] This is illustrated by the spent Au/TiO_2 catalyst, for which a second C 1s peak at 286.25 eV is observed, assigned to C−O bond containing carbon species.[42] If the C 1s reference peak of the TiO_2 catalysts would be higher than 284.8 eV, this would imply that the determined BE is too small, causing negative BE shifts with respect to the gold reference. The use of Ti $2p_{3/2}$ as reference may also result in small shifts as Ti^{4+} can be reduced in situ to Ti^{3+}. Therefore, it is concluded that the use of C1s as reference is not a good measure for chemical state of the gold particle.

Comparable to the IS-QS plots for gold compounds studied with Mössbauer, combinations of photoelectron and Auger lines are more indicative of the chemical state[18] than the photoelectron line alone. Use of an unmonochromatized X-ray source renders it possible to generate Auger electrons. Generally, these lines are overlooked, as it is a relatively weak phenomenon and, for example, the Au $M_5N_{67}N_{67}$ are observed in the negative BE region (1253.6−2015 = −761.4 eV).[19]

As the oxidation state of the gold may change as a function of distance from the surface, the penetration depth of both photoelectron and Auger electrons is important. The kinetic energy of the Au $4f_{7/2}$ electrons (1253.6−84.0 = 1169.6 eV) implies an inelastic mean free path (IMFP) of 1.4 nm, whereas for the Au $M_5N_{67}N_{67}$ Auger electrons (2015 eV), an IMFP of 2.2 nm is reported.[43] Therefore, mostly the surface atoms of the 5 nm gold particles will appear in the XPS spectra. As the

Auger electrons have a similar IMFP, combinations of Au $4f_{7/2}$ and Auger electrons will yield information on the same surface species.

Only samples containing more than 1 wt % Au can be used to determine the Auger lines. Ideally, both 1 and 10 wt % Au catalysts with identical particle sizes and catalytic properties should be prepared. Both the 1 and 10 wt % Au/TiO_2 catalyst prepared via tetrakis(hydroxymethyl)phosphonium chloride (THPC) show no epoxidation activity. The gold particle size is comparable to the active Au/TiO_2-based catalysts prepared via deposition−precipitation. Therefore, the inactivity may be due to the P remaining after calcination at 673 K. This has been indicated in the literature[16] and P is observed in the XPS spectrum. Whether the remaining P is related to Au or to the Ti epoxidation center cannot be deducted from the XPS data. No profound differences for the Au and O intensities are observed. Apparently, the poly(vinylpyrrolidone) (PVP) used for the other colloid can be removed sufficiently during calcination at 673 K. In this case, no evidence has been found in XPS for remaining nitrogen (oxide) species.

It is noteworthy that no difference in Au 4f BE is observed before and after reaction for the Au/TiO_2 catalyst calcined at 673 K. This indicates that the slight changes observed in (IS,QS) of the metallic surface species are not significant and supports the conclusion that deactivation is due to the TiO_2 support.[4]

For the 10 wt % Au samples, the XPS and Auger spectra (Figure 7) allow determination of the Auger parameter α. As given in Table 3, α shows a shift for the active 10 wt % (PVP) Au/TiO_2 catalyst of −0.27 eV with respect to the Au reference (α = 2099.15 eV), whereas for the THPC sample, only −0.07 eV is found. The difference between the two catalysts is mainly due to the difference in Auger line position. The value of 84.05 eV obtained for the Au reference is in good agreement with literature (84.00 eV).[23]

The 1 wt % Au/TiO_2 and the 10 wt % (PVP) Au/TiO_2 are both calcined at 673 K and active in propene epoxidation. TEM indicated a similar particle size distribution. Therefore, it is concluded that the active gold species of these two catalysts are similar. From the $4f_{7/2}$ BE of the 1 wt % Au/TiO_2, a shift of −0.76 eV with respect to the measured gold reference is observed, whereas the Auger parameter of the active 10 wt % (PVP) Au/TiO_2 catalyst gives a shift of only −0.27 eV.

Analysis of the Auger parameter will not suffer from charging of the gold particle as the photoelectron and the Auger electron are related to the same gold species. Furthermore, a change in the Auger parameter compared to the gold reference is indicative of final state effects.[21,44] This would imply that the Au $4f_{7/2}$ BE of the studied gold particles would be higher than the 84.00 eV reported for metallic gold. The real value of BE can even be higher if charging of the gold particle occurs, whereas the occurrence of initial state effects would decrease the BE.[21] As the real BE value is not known, both the influence of initial state effects and charging cannot be elucidated.

The value of −0.27 eV for the shift in Auger parameter should be compared with a range from −1.30 eV up to −0.12 eV that has been reported for gold particles of increasing size on yttria-stabilized ZrO_2.[21] In this study, it has been shown that for small gold particles initial state effects are important, whereas for larger gold particles, final state effects will give nonmetallic BE. These larger gold particles have a shift in Auger parameter of −0.36 eV up to −0.12 eV. Unfortunately, no results on gold particle sizes were reported. Dalacu and coworkers[40] showed that initial state effects start to appear at sizes below 2 nm.

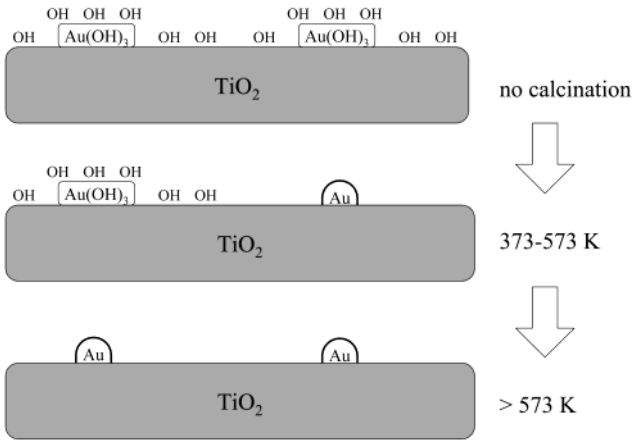

Figure 10. Schematic impression of conversion of $Au(OH)_3$ species supported on TiO_2 into Au/TiO_2 during calcination.

In conclusion, the shift in Auger parameter is within the range of what is reported for metallic gold particles. Therefore, the negative shift is not related to the gold particles being negatively charged but to the increased fraction of surface atoms. These surface atoms are less coordinated and exhibit reduced screening of the photoelectron core hole. For elucidation of chemical state of the gold (for example the Au/TiO_2 catalyst calcined at 423 and 673 K), either the Auger parameter or a metallic gold sample with a comparable dispersion should be used.

On the basis of the XPS and Auger data, the 10 wt % (THPC) Au/TiO_2 sample is expected to have either larger gold particles (not supported by TEM and MAS, not shown here) or an increased coordination of the surface atoms and, therefore, an enhanced screening. The latter option is supported by the presence of P in this sample, which may be coordinated to Au, thereby reducing its propene epoxidation activity.

Figure 4 and Table 3 show that also the 1 wt % Au/TiO_2 calcined at 423 K has a Au 4f BE of 84.21 eV, which would imply mostly metallic gold. However, a better reference in this respect is the 1 wt % Au/TiO_2 calcined at 673 K. Compared to the latter sample, the catalyst calcined at 423 K has a 0.92 eV higher BE. On the basis of the discussion in the previous paragraphs, this would either imply a difference in gold particle size or a more oxidized gold species. TEM indicates that the mean gold particle size is comparable, and therefore, the higher BE is assigned to oxidized gold. Park and Lee reported 2.4 and 3.8 eV relative to Au metal for Au_2O_3 and $Au(OH)_3$, respectively,[36] but also 1.9 eV for $Au(OH)_3$ is stated in the literature.[45] The surface sensitivity of XPS is nicely illustrated by Figure 4 and Table 1 for the Au/TiO_2 catalyst calcined at 423 K. Although in MAS 36% of the spectrum consists of metallic gold particles and their metallic surface atoms, XPS mainly detects the oxidized gold species. This indicates the oxidized gold species is highly dispersed, probably in the form of the $Au(OH)_3$ moieties that were previously proposed.

A schematic picture of the phases present during preparation of Au/TiO_2 catalysts is given in Figure 10. After the deposition-precipitation of $Au(OH)_3$ on TiO_2, during calcination, gold is reduced and water is removed by dehydroxylation. The temperature dependence of the Au metal particle formation is probably due to the different crystal phases and surfaces that are present in TiO_2 P25. After calcination treatments at temperatures above 573 K and for gold particles larger than 3 nm, all gold is present in a metallic form. Both XPS and MAS show the presence of metallic gold surface atoms after high-temperature calcination.

It is shown that both XPS and MAS are excellent tools in the characterization of catalysts with nanosized gold particles. Therefore, both MAS and Auger parameter analysis can play an important role in the elucidation of gold particle size effects in propene epoxidation but also for CO oxidation. Application of higher gold loadings enhances MAS sensitivity and enables the determination of the Auger parameter. Future challenges are, therefore, the preparation of higher gold loaded samples with a uniform gold particle size around 2 nm. Correlation of catalytic activity with different gold particle sizes will then be possible. Colloid preparation routes may be a valuable tool in this respect, although these will not always yield catalytically active samples.

Conclusion

Au/TiO_2-based propene epoxidation catalysts (1 wt.%) calcined at 673 K have been characterized by TEM, XPS, and ^{197}Au MAS. Gold particle sizes ranged from 3 to 6 nm. All techniques indicate that metallic gold was the active phase during propene epoxidation over these catalysts. The two Au species found in Mössbauer spectra were assigned to Au atoms in the core of a metal particle and metallic gold on the outer surface of a metal particle. On the basis of TEM analysis, it was shown that the surface atoms have a smaller recoil-free fraction because of their lower coordination. For Au/TiO_2, it was observed that during calcination $Au(OH)_3$ species formed after deposition−precipitation are converted into metallic gold. Gold particles were shown not to grow gradually during calcination, and it is tentatively concluded that the conversion of $Au(OH)_3$ moieties occurs simultaneously with dehydroxylation of the TiO_2 support.

Both 1 and 10 wt % gold catalysts with similar particle size have been prepared via a colloid route. The use of poly(vinylpyrrolidone) (PVP) in the colloid synthesis yielded active epoxidation catalysts. XPS analysis showed that Au $4f_{7/2}$ binding energy based on the C 1s reference should be interpreted with caution. Determination of the Auger parameter of 10 wt % Au catalysts confirmed that the surface layer of 3−5 nm gold particles is metallic. The negative shift in Auger parameter with respect to metallic bulk gold has to be related to final state effects. These effects are due to the less coordinated but metallic gold surface atoms which exhibit reduced screening.

Acknowledgment. Financial support by Synetix and Huntsman Specialty Chemicals is gratefully acknowledged. Dr. Patricia J. Kooyman of the National Centre for High Resolution Electron Microscopy, Delft University of Technology, Delft, The Netherlands is acknowledged for performing the electron microscopy investigations.

References and Notes

(1) Bond, G. C.; Thompson, D. T. *Catal. Rev. Sci. Eng.* **1999**, *43*, 319.
(2) Haruta, M. *Catal. Today* **1997**, *36*, 153.
(3) Nijhuis, T. A.; Huizinga, B. J.; Makkee, M.; Moulijn, J. A. *Ind. Eng. Chem. Res.* **1999**, *38*, 884.
(4) Mul, G.; Zwijnenburg, A.; van der Linden, B.; Makkee, M.; Moulijn, J. A. *J. Catal.* **2001**, *201*, 128.
(5) Schubert, M. M.; Hackenberg, S.; van Veen, A. C.; Muhler, M.; Plzak, V.; Behm, R. J. *J. Catal.* **2001**, *197*, 113.
(6) Valden, M.; Pak, S.; Lai, X.; Goodman, D. W. *Catal. Lett.* **1998**, *56*, 7.
(7) Chusuei, C. C.; Lai, X.; Luo, K.; Goodman, D. W. *Topics Catal.* **2001**, *14*, 71.
(8) Kuperman, A.; Bowman, R. G.; Clark, H. W.; Hartwell, G. E.; Schoeman, B. J.; Tuinstra, H. E.; Meima, G. R. U.S. Patent 6,255,499, 2001.
(9) Kuperman, A.; Bowman, R. G.; Hartwell, G. E.; Schoeman, B. J.; Tuinstra, H. E.; Meima, G. R. WO Patent 00/59632, 2000.
(10) Grunwaldt, J.-D.; Baiker, A. *J. Phys. Chem. B* **1999**, *103*, 1002.
(11) Stangland, E. E.; Stavens, K. B.; Andres, R. P.; Delgass, W. N. *J. Catal.* **2000**, *191*, 332.
(12) Finch, R. M.; Hodge, N. A.; Hutchings, G. J.; Meagher, A.; Pankhurst, Q. A.; Siddiqui, M. R. H.; Wagner, F. E.; Whyman, R. *Phys. Chem. Chem. Phys.* **1999**, *1*, 485.
(13) Wagner, F. E.; Galvagno, S.; Milone, C.; Visco, A. M.; Stievano, L.; Calogero, S. *J. Chem. Soc., Faraday Trans.* **1997**, *93*, 3403.
(14) Kobayashi, Y.; Nasu, S.; Tsubota, S.; Haruta, M. *Hyperfine Interact.* **2000**, *126*, 95.
(15) Paulus, P. M.; Goossens, A.; Thiel, R. C.; Schmid, G.; van der Kraan, A. M.; de Jongh, L. J. *Hyperfine Interact.* **2000**, *126*, 199.
(16) Grunwaldt, J.-D.; Kiener, C.; Baiker, A. *J. Catal.* **1999**, *181*, 223.
(17) Porta, F.; Prati, L.; Rossi, M.; Coluccia, S.; Martra, G. *Catal. Today* **2000**, *61*, 165.
(18) Wagner, C. D.; Gale, L. H.; Raymond, R. H. *Anal. Chem.* **1979**, *51*, 466.
(19) Castle, J. E.; West, R. H. *J. Electron Spectrosc. Relat. Phenom.* **1979**, *16*, 195.
(20) *Surf. Interface Anal.* **1991**, *17*, 889.
(21) Zafeiratos, S.; Kennou, S. *Surf. Sci.* **1999**, *443*, 238.
(22) Goossens, A.; Crajé, M. W. J.; van der Kraan, A. M.; Zwijnenburg, A.; Makkee, M.; Moulijn, J. A.; de Jongh, L. J. *Catal. Today* **2002**, *72*, 95.
(23) Wagner, C. D.; Naumkin, A. V.; Kraut-Vass, A.; Allison, J. W.; Powell, C. J.; Rumble, J. R., *NIST X-ray Photoelectron Spectroscopy Database*, National Institute of Standards and Technology: Gaithersburg, MD, 2001, http://srdata.nist.gov/xps/ (accessed October 2001).
(24) Mie, G. *Ann. Phys.* **1908**, *4*, 377.
(25) Parish, R. V. In *Mössbauer Spectroscopy Applied to Inorganic Chemistry*; Long, G. J., Eds.; Plenum Press: New York, 1984; pp 577−617.
(26) Faltens, M. O.; Shirley, D. A. *J. Chem. Phys.* **1970**, *53*, 4249.
(27) Murphy, P.; Stevens, G.; LaGrange, M. S. *Geochim. Cosmochim. Acta* **2000**, *64*, 479.
(28) Viegers, M. P. A.; Trooster, J. M. *Phys. Rev. B* **1977**, *15*, 72.
(29) Mulder, F. M.; Thiel, R. C.; de Jongh, L. J.; Gubbens, P. C. M. *Nanostruct. Mater.* **1996**, *7*, 269.
(30) Paulus, P. M.; Goossens, A.; Thiel, R. C.; van der Kraan, A. M.; Schmid, G.; de Jongh, L. J. *Phys. Rev. B* **2001**, *64*, 205418−1.
(31) Stievano, L.; Santucci, S.; Lozzi, L.; Calogero, S.; Wagner, F. E. *J. Non-Cryst. Sol.* **1998**, *232−234*, 644.
(32) Bond, G. C.; Thompson, D. T. *Gold Bull.* **2000**, *33*, 41.
(33) Geus, J. W. In *Preparation of Catalysts III*; Poncelet, G., Grange, P., Jacobs, P. A., Eds.; Elsevier Science Publishers B. V.: Amsterdam, 1983; pp 1−33.
(34) Blick, K.; Mitrelias, T. D.; Hargreaves, J. S. J.; Hutchings, G. J.; Joyner, R. W.; Kiely, C. J.; Wagner, F. E. *Catal. Lett.* **1998**, *50*, 211.
(35) Haruta, M.; Tsubota, S.; Kobayashi, T.; Kageyama, H.; Genet, M. J.; Delmon, B. *J. Catal.* **1993**, *144*, 175.
(36) Park, E. D.; Lee, J. S. *J. Catal.* **1999**, *186*, 1.
(37) Paulus, P. M. *Nanometer-sized metal particles studied by Mössbauer effect spectroscopy and magnetic probes*, Ph.D. Thesis, Universiteit Leiden, Leiden, The Netherlands, 2000.
(38) Horváth, A.; Toth, L.; Guczi, L. *Catal. Lett.* **2000**, *67*, 117.
(39) Claus, P.; Brückner, A.; Mohr, C.; Hofmeister, H. *J. Am. Chem. Soc.* **2000**, *122*, 11430.
(40) Dalacu, D.; Klemberg-Sapieha, J. E.; Martinu, L. *Surf. Sci.* **2001**, *472*, 33.
(41) Citrin, P.; Wertheim, G. K.; Baer, Y. *Phys. Rev. B* **1983**, *27*, 3160.
(42) Hontoria-Lucas, C.; López-Peinado, A. J.; López-González, J. d. D.; Rojas-Cervantes, M. L.; Martín-Aranda, R. M. *Carbon* **2001**, *33*, 1585.
(43) Tanuma, S.; Powell, C. J.; Penn, D. R. *Surf. Interface Anal.* **1991**, *17*, 911.
(44) Kohiki, S. *Appl. Surf. Sci.* **1986**, *25*, 81.
(45) Juodkazis, K.; Juodkazyte, J.; Jasulaitiene, V.; Lukinskas, A.; Sebeka, B. *Electrochem. Commun.* **2000**, *2*, 503.